WPS1-CPR(18) 18886

A Ali et al.

Initial Results from the Hotspot Detection Scheme for Protection of Plasma Facing Components in Wendelstein 7-X

Preprint of Paper to be submitted for publication in Proceeding of 23rd International Conference on Plasma Surface Interactions in Controlled Fusion Devices (PSI-23)

This work has been carried out within the framework of the EUROfusion Consortium and has received funding from the Euratom research and training programme 2014-2018 under grant agreement No 633053. The views and opinions expressed herein do not necessarily reflect those of the European Commission.

Initial Results from the Hotspot Detection Scheme for Protection of Plasma Facing Components in Wendelstein 7-X

A. Ali[a,c], M. Jakubowski[a], H. Niemann[a], Y. Corre[g], P. Drewelow[a], A. Puig Sitjes[a], R. Neu[b,c], T. Sunn Pedersen[a], F. Pisano[e], Y. Gao[d], G. Wurden[f], the W7-X Team[a]

[a] *Max-Planck-Institut für Plasmaphysik, Wendelsteinstr. 1, 17491 Greifswald, Germany*
[b] *Max-Planck-Institut für Plasmaphysik, Boltzmannstr. 2, 85748 Garching, Germany*
[c] *TUM, Department of Mechanical Engineering, Boltzmannstra. 15, 85748 Garching, Germany*
[d] *Forschungszentrum Jülich GmbH, 52425 Jülich, Germany*
[e] *University of Cagliari, 09124 Cagliari, Italy*
[f] *Los Alamos National Laboratory, 85748 Los Alamos, USA*
[g] *CEA, IRFM, F-13108 Saint-Paul-Lez-Durance, France.*

Abstract

One of the main aims of Wendelstein 7-X (W7-X), an advanced stellarator, is to investigate the quasi-steady state operation of magnetic confinement devices for nuclear fusion, for which power exhaust is an important issue. A predominant fraction of the energy leaving from the confined plasma region will be removed by 10 so-called island divertors, which are designed to sustain a maximum heat flux of up to $10\,\mathrm{MW\,m^{-2}}$. An essential prerequisite for the safe operation of a steady-state device is automatic detection of the hot spots and other abnormal events. Simple temperature limits in infrared (IR) thermographic images might get misguided by hotspots. To protect the divertor elements from overheating, and to monitor power deposition onto the divertor elements, near real-time hotspot detection algorithms for the analysis of carbon plasma facing components (PFCs) were implemented and tested at GLADIS.

One of the difficulties in the hotspot detection in a carbon-based machine is the deposition of the plasma impurities as layers with a reduced thermal connection to the underlying bulk material. We have developed and successfully tested a method to classify surface layers and benchmark the performance of the method with the Tore Supra IR data operating with actively cooled carbon PFCs. The surface layers can be detected in a steady plasma discharge during the initial rise and decay in temperature when a strike line touches the parts of the divertor or wall. It can also be detected by modulating electron cyclotron resonance heating (ECRH) input power. This feature allows detecting overheated areas while reducing false positives. For the recent operational campaign, inertially cooled test divertor units (TDU) were installed to prepare the steady-state operation with water-cooled divertor units. We were able to present automatic, near real-time detection of hot spots and identification of surface layers on W7-X divertor. The results were compared with a best fit estimate of the heat transmission coefficient α which is used to calculate heat flux onto the divertor in the presence of surface layers.

Keywords: W7-X, stellarator, divertor, THEODOR, TDU, PFCs, TS, TPL, GLADIS

1. Introduction

W7-X is an optimized stellarator, designed for steady-state operation of up to 30 minutes. The PFCs which are subject to most substantial power loads are 10 divertor units. The divertor of W7-X is subdivided into units which are composed of about 890 PFCs covered with about 14000 flat tiles of carbon fiber composite (CFC) NB31 [1]. These CFC armor tiles are bonded via an Active Metal Casting copper (AMC-Cu) interlayer to a copper chromium zirconium (CuCrZr) cooling structure as seen in Figure 1. The Cu interlayer (so-called bi-layer) is used to reduce stresses and strains in both the CFC area as well as the metallic section [2].

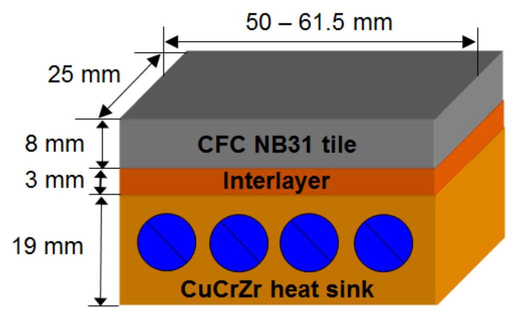

Figure 1: Graphical design of CFC tile. The gray surface on the top is composed of CFC NB31 type bulk surface connected to CuCrZr cooling structure with the help of Cu interlayer.

*Corresponding author
Email address: adnan.ali@ipp.mpg.de (the W7-X Team)

A possible overheating of PFCs may lead to defects at the bonding of the CFC tiles to the Active Metal Casting (AMC) interlayer [3]. Thus, it is required to detect such defects in near real-time during plasma operation to reduce the local heat if required. Such systems to prevent overheating of PFCs are also developed in other fusion devices, e.g., JET [4] and ASDEX Upgrade [5].

Each divertor module at W7-X consists of 250 mm to 500 mm long and 50 mm to 61.5 mm wide individual target elements. In the recent campaign of W7-X, inertially cooled carbon-based test divertor units (TDU) are installed. The TDU divertor shape has a similar structure as the water-cooled divertor for the preparation of steady-state operations.

2. W7-X Hotspot Detection Scheme

Infrared Diagnostic at W7-X. An infrared (IR) camera with a spectral wavelength range of 3 µm to 5 µm is mounted inside the prototype endoscope [6]. The optical setup of the prototype endoscope makes it possible to cover the entire view of the divertor in one of the module as can be seen in Figure 2. The integration time of the IR camera is varied from 50 µs to 200 µs depending on the expected surface temperature on the divertor. A control software mentioned in [7, 8] with a dedicated acquisition workstation was used to control the camera and acquire results from the graphics processing unit (GPU).

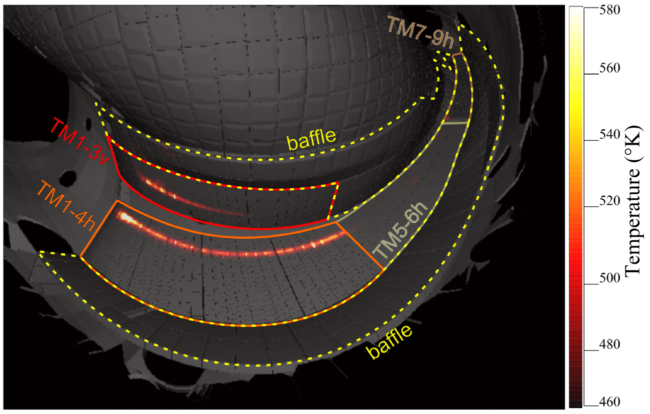

Figure 2: Scene model showing lower divertor mapped to IR temperature data in kelvin (K°). The horizontal divertor range from target module 1 to 9 (TM1-9h) and vertical divertor from 1 to 3 (TM1-3v).

Hotspots. The primary strategy of the W7-X IR imaging diagnostic is to detect hot spots on the carbon plasma facing components and thermal event recognition [7, 8]. Hot spots due to excessive power loads on the materials can reduce the heat transfer from the bulk to the cooling channel. Also, they can damage the upper surface of the material which can lead to cracks in the structure. They can also appear because of delamination in the water-cooled tile [3, 7] and needs to be clearly distinguished from overheating due to surface layers to avoid false alarms. That is why they are required to be detected in near real time to provide early response to the central control system of W7-X [3].

Surface Layers. In general, the composition of the local distribution of impurity depositions like carbon, hydrogen, oxygen, boron or iron contribute to the build-up of surface layers. Due to weaker thermal connection to the bulk material, the areas where impurities are re-deposited appear to be at a higher temperature and could be interpreted as hot spots. In all the fusion related plasma confinement experiments, classification and detection of IR emission because of erosion and re-deposition during the interaction of plasma with the material is in-depth investigated [9]. Such investigation is necessary regarding safety diagnostics since it can lead to uncertainties in the thermographic monitoring and heat flux calculation which has already been observed on W7-AS [10, 11]. The heat fluxes were partially overestimated up to a factor of 4 during the W7-AS operation [11].

Numerical Method. For simulating the behavior of surface layers, on the W7-X PFCs, FEM simulations were conducted, by overlaying a un-connected layer on top of the bulk surface [12]. The principle behavior of temperature evolution of PFCs with and without surface layers is shown in Figure 3.

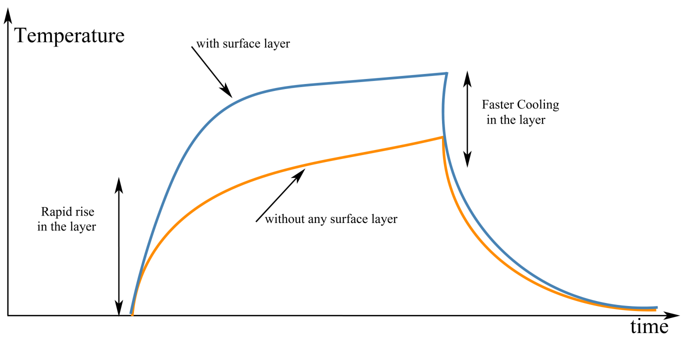

Figure 3: Schematic of a temperature evolution of a PFC show with (red) and without (green) surface layers.

The apparent temperature on the area where surface layers are present increases much faster as compared to a clean surface whereas during the cooling phase, the energy is dissipated much faster in the form of radiation, which is why the surface layers cool down much faster as compared to a clean surface. A numerical method based on the normalized derivative of the temperature profile for detecting surface layers is developed that is defined in equation (1) as

$$\mathrm{norm}_{[\mathrm{t,T}]} = \frac{\partial_t T(t)}{T(t)}, \tag{1}$$

where T(t) is the surface temperature of a tile and $\partial_t T(t)$ is the partial derivative of temperature during the initial and decay phase. The $\mathrm{norm}_{[\mathrm{t,\ T}]}$ of a surface layer will be higher during the initial rise time and lower during the initial decay time as compared to a clean surface that is without any deposition of layers. A user-defined threshold on $norm_{[t,\,T]}$ is used to identify areas with surface layers during the plasma operation. The algorithm is created using the CUDA library for graphics processing unit (GPU) computation. The usage of GPU increases the performance of the numerical method for large datasets of thermographic images. Significant enhancement in the performance of the method by a factor of 100 was achieved as compared to its initial state as mentioned in [7].

Tore Supra Limiter . For bench-marking the numerical method to detect the areas where surface layers are present on water-cooled PFCs, thermographic data of Tore Supra (TS) looking at the Toroidal Pump Limiter (TPL) was analyzed. The TPL is made of 6 mm thick CFC tiles assembled on CuCrZr actively cooled body (thus based on the same technology as foreseen in the W7-X divertor modules). The TS-IR endoscopes were equipped with two IR cameras with spectral wavelength range of 3 µm to 5 µm. Three viewing lines, two for 2 sections of 35° of the TPL located at the bottom of the machine and one line looking at the heating antenna were observed [13]. The spatial resolution on the TPL was between 7 mm to 10 mm in the center and outer part of the image respectively. For a standard TS plasma discharge (2 MW injected power, 1 MA plasma current), healthy PFC located in net erosion area (with no surface layer) have maximum surface temperatures of around 350 °C. The part of the limiter with surface layers, located mainly at the periphery of the erosion areas, shows higher surface temperatures of more than 650 °C which can be seen in Figure 4.

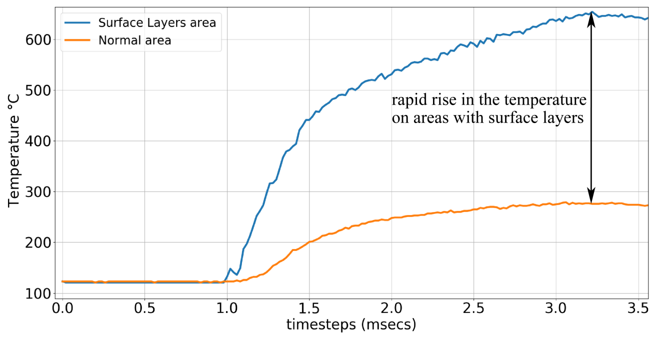

Figure 4: Surface temperature evolution of two different areas on TPL as shown in Figure 6a. The blue curve shows the maximum temperature on the areas where surface layers are expected. The orange curve show the area where no surface layers are expected.

The $norm_{[t,\,T]}$ on the areas where surface layers are expected is higher as compared to a normal surface area which can be seen in Figure 5. In the current case, the user-defined threshold of $norm_{[t,\,T]}$ for the areas with surface layers was set to a value of 7. The surface layers results from TS data can be seen in Figure 6. The two ROIs used to extract the temperature evolution used in Figure 4 and Figure 5 are shown in Figure 6a.

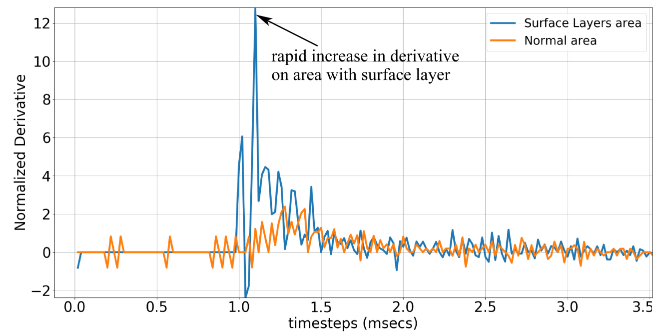

Figure 5: $norm_{[t,\,T]}$ for areas where the surface layers are expected is shown in blue and normal surface in orange.

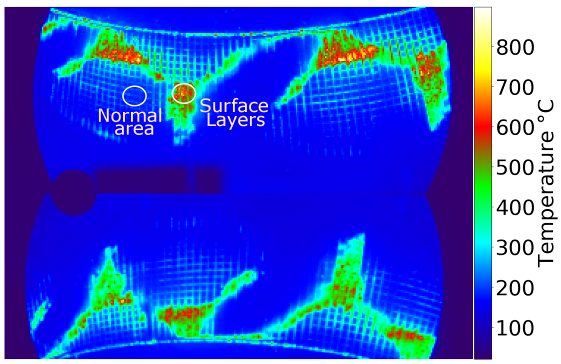

(a) Surface Temperature on the Tore Supra Limiter

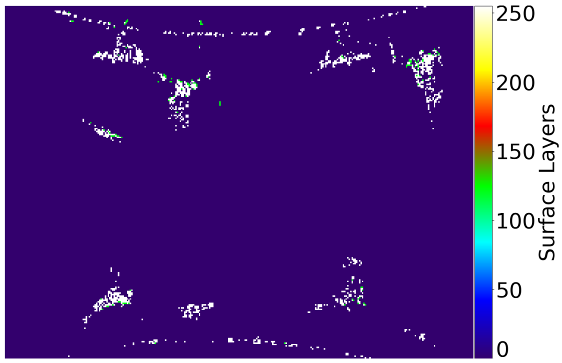

(b) Surface Layers detected by the numerical method

Figure 6: Results from Tore Supra showing surface temperature on the TPL taken from an IR camera. Figure 6b show detected surface layers during rise (white) and (green) decay time.

The surface layer detected by the algorithm shows good agreement with visual inspection and previous IR data analysis [9, 14]. These observations were the first successful application which verified that the numerical method can be used to detect the surface layers inside a nuclear fusion reactor.

3. Comparison of Methods used for detecting Surface Layers at W7-X.

To obtain the heat flux on the divertor targets, information about surface temperature, spatial calibration, and the material properties are necessary requirements. If these parameters are available, the heat flux can be calculated using the heat diffusion equation using THEODOR (THermal Energy Onto DivertOR) code[15]. Further details regarding the heat flux calculation can be found in [5, 15, 16, 17]. The most common practice for refining the heat flux calculation in the presence of surface layers is by estimating the heat transmission coefficient α in $\mathrm{W\,m^{-2}\,K^{-1}}$ which is defined in equation (2) as

$$\alpha = \frac{\lambda_{\text{layer}}}{d_{\text{layer}}}, \tag{2}$$

where λ_{layer} is the heat conductivity of the layer and d_{layer} is the thickness of the layer. Further details regarding the heat transmission coefficient α can be seen in [18]. Small values of α reflect weakly coupled (small λ_{layer}) or thick (large d_{layer}) surface layers. As the layer thickness and heat conductivity are unknown parameters, α is estimated iteratively. Too high values of α usually result in overestimated heat fluxes during the plasma discharge and negative heat fluxes at the end. Since the actual heat flux during an experiment is unknown, only the negative minimal heat flux at the end can be used to assess the quality of the assumed α value. The iteration thus follows:

$$\alpha_{i+1}(s) = \alpha_i(s) b_i^{\epsilon(s)}, \tag{3}$$

where $b_i = 1 + b/\sqrt{i}$ reduces after each step. The free parameter b (here set to 0.5) controls the convergence speed and the resilience against numerical fluctuations. How strong α is adjusted in the next iteration depends on $\epsilon(s)$ as the ratio between the minimal (negative) heat flux at this point and absolute value of the most extreme minima along a profile. As a stop criteria for the iterations, it is assumed that the residual negative minima amount to less than 1 % of the observed maximal heat flux. In the current state, the limit is set to 200 iterations.

$$\frac{|q_{\text{min}-\text{low}}|}{\max(q_{\text{max}-\text{high}}(s))} < 1\,\%. \tag{4}$$

The iterative method to find α is computationally expensive [18]. This feature restricts the usage of the method for real-time applications and is the main reason for adapting a faster method of estimation of the layers. To compare the results obtained from the numerical method to detect surface layers as mentioned in equation (1), it was compared with the heat transmission coefficient α obtained from the heat flux calculation. The α values can be used to identify areas where surface layers affect the heat flux calculation.

The values of α obtained from the iterative method as mentioned in equation (3) are projected on the 2D model as seen in Figure 7b. The darker blue areas in Figure 7b show small values of α where surface layers are expected, whereas the light blue area shows normal surfaces where

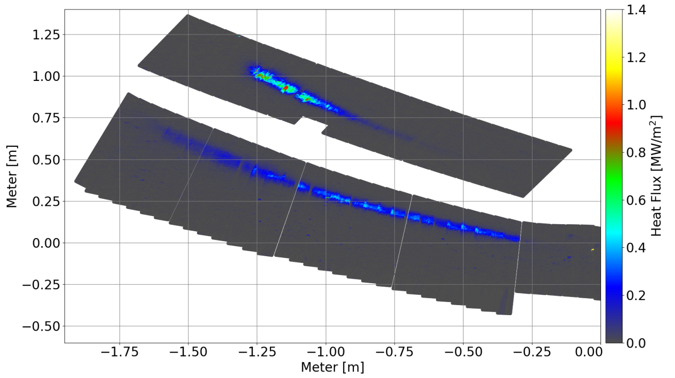

(a) Projection of the heat flux mapped on the horizontal and vertical divertor of W7-X. The maximum heat flux on the vertical divertor is more than $1\,\mathrm{MW/m^2}$.

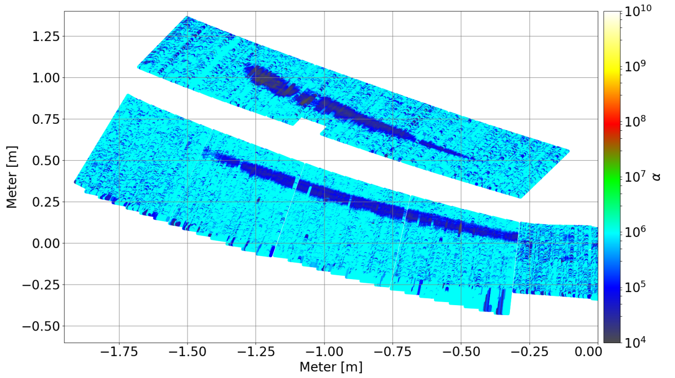

(b) Projection of heat tranmission coefficient α on the horizontal and vertical divertor. The dark blue color shows lower values of α which correspond to the location of surface layers. The values of α below 5×10^5 are linked to surface layers.

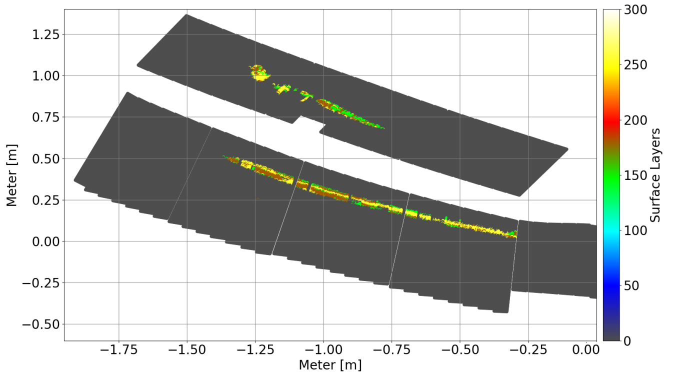

(c) Projection of surface layers detected on the W7-X horizontal and vertical divertor by the numerical method implemented in GPU. The yellow color shows the position of surface layers detected during the rise time. The brown color show areas where surface layers are detected during the rise and decay time. The green show layers detected only during the decay time.

Figure 7: Comparison of α values from the heat flux calculation and the surface layer results from numerical algorithm mapped to a simplified 2D model of the W7-X divertor for shot number #20171101.012.

no deposition was estimated. The surface layer result obtained from the numerical method in equation (1) which is processed in GPU is projected on a simplified 2D model of the divertor as seen in Figure 7c. The control software [7, 8] computes the numerical method and classifies the surface layers based on the state when they were detected.

The results of the two numerical methods for detecting the surface layers as shown in Figures 7b and 7c are overlayed to find the matching areas. This overlaying provides meaningful information to find the best threshold for $\mathrm{norm}_{[\mathrm{t},\ \mathrm{T}]}$, which matches well with the regions of lower α values. The histogram of α on the areas where the numerical method detected surface layers can be seen in Figure 8.

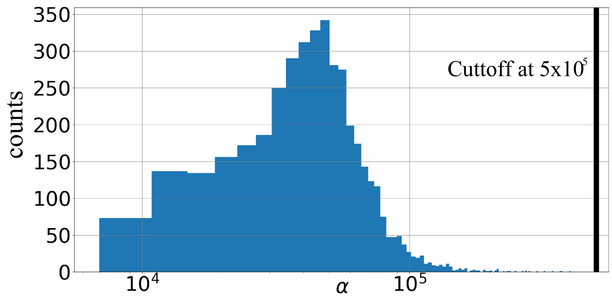

Figure 8: Histogram showing the distribution of α values on the areas which matches with the surface layers detected by the numerical algorithm for shot number #20171101.012. The cutoff range for the minimum value of α for surface layers is set as 5×10^5 .

The majority (90 % to 99 % in most cases) of α values lies below 5×10^5, which is used as a cut-off range for the region with surface layers. The results achieved from the analysis prove that the numerical method can be used alternatively to find areas that have low α values and by that indicates the presence of surface layers.

It is important to mention here that these results show the comparison of areas where the surface layers are detected by the numerical method which matches with the α values in those locations and the inverse is not proven yet. There can be areas where the α correction method detected surface layers and the numerical method was not able to successfully detect them. However, this difference is still under further analysis to find an optimal way to resolve this issue.

The numerical method depends on the relative background offset level (roughly 20 K above the background noise level) which may change during the day. In some cases, the numerical method is unable to detect surface layers which require further analysis. This failure can be either due to lower heating of the divertor surface (temperature values lying below the offset level), low thickness of the surface layers or due to $\mathrm{norm}_{[\mathrm{t},\ \mathrm{T}]}$ values lower than the criterion parameters. The lower values of $\mathrm{norm}_{[\mathrm{t},\ \mathrm{T}]}$ can be due to rise in the background temperature during the day. However the influence of background temperature will reduce significantly in the future campaigns when water cooled PFCs will be installed.

4. Outlook and Summary

In this work, we presented the experimental performance of the near real-time system for detection of hotspots and in particular the automatic identification of surface layers, due to erosion and re-deposition of armor carbon tiles of the W7-X divertor. The numerical method shows promising results to detect surface layers on the carbon-based test divertor unit in W7-X. The results from the numerical method computed by GPU is compared with the α values obtained from the heat flux calculation. The numerical method was successfully validated on water-cooled PFCs using the thermal images from Tore Supra.

Acknowledgment

This work has been carried out within the framework of the EUROfusion Consortium and has received funding from the Euratom research and training programme 2014-2018 under grant agreement No 633053. The views and opinions expressed herein do not necessarily reflect those of the European Commission.

References

[1] G. Pintsuk, J. Compan, J. Linke, P. Majerus, A. Peacock, D. Pitzer, M. Rödig, Mechanical and thermo-physical characterization of the carbon fibre composite NB31, Phys. Scr. T T128 (2007) 66–71.

[2] H. Greuner, B. Böswirth, J. Boscary, P. Chaudhuri, J. Schlosser, T. Friedrich, A. Plankensteiner, R. Tivey, Cyclic heat load testing of improved CFC/Cu bonding for the W7-X divertor targets, J. Nucl. Mater. 386-388 (2009) 772–775.

[3] A. Rodatos, H. Greuner, M. W. Jakubowski, J. Boscary, G. A. Wurden, T. S. Pedersen, R. König, Detecting divertor damage during steady state operation of Wendelstein 7-X from thermographic measurements, Rev. Sci. Instrum. 87 (2016) 1–8.

[4] G. Arnoux, S. Devaux, D. Alves, I. Balboa, C. Balorin, N. Balshaw, M. Beldishevski, P. Carvalho, M. Clever, S. Cramp, J. L. De Pablos, E. De La Cal, D. Falie, P. Garcia-Sanchez, R. Felton, V. Gervaise, A. Goodyear, A. Horton, S. Jachmich, A. Huber, M. Jouve, D. Kinna, U. Kruezi, A. Manzanares, V. Martin, P. McCullen, V. Moncada, K. Obrejan, K. Patel, P. J. Lomas, A. Neto, F. Rimini, C. Ruset, B. Schweer, G. Sergienko, B. Sieglin, A. Soleto, M. Stamp, A. Stephen, P. D. Thomas, D. F. Valcárcel, J. Williams, J. Wilson, K. D. Zastrow, A protection system for the JET ITER-like wall based on imaging diagnostics, Rev. Sci. Instrum. 83 (2012).

[5] B. Sieglin, M. Faitsch, A. Herrmann, S. Martinov, T. Eich, Real-time infrared thermography at ASDEX Upgrade, Fusion Sci. Technol. 69 (2016) 580–585.

[6] M. W. Jakubowski, C. Biedermann, R. König, A. Lorenz, T. Sunn Pedersen, A. Rodatos, Development of infrared and visible endoscope as the safety diagnostic for steady- state operation of Wendelstein 7-X, QIRT 100 (2014).

[7] A. Ali, M. Jakubowski, H. Greuner, B. Böswirth, V. Moncada, A. P. Sitjes, R. Neu, T. S. Pedersen, W7-X. Team, Experimental results of near real-time protection system for plasma facing components in Wendelstein 7-X at GLADIS, Phys. Scr. T170 (2017).

[8] A. Puig Sitjes, M. Jakubowski, A. Ali, P. Drewelow, V. Moncada, F. Pisano, T. T. Ngo, B. Cannas, J. M. Travere, G. Kocsis, T. Szepesi, T. Szabolics, W7-X. Team, Wendelstein 7-X Near Real-Time Image Diagnostic System for Plasma-Facing Components Protection, Fusion Sci. Technol. 00 (2017) 1–9.

[9] Y. Corre, C. Brosset, E. Dufour, D. Guilhem, C. Lowry, R. Mitteau, P. Monier-Garbet, B. Pegourie, E. Tsitrone, S. Vallet, Visualisation of the deposited layer on the Toroidal Pumped Limiter of Tore Supra using IR data during disruptions, 32nd EPS Conf. Control. Fusion Plasma Physics. Contrib. Pap. 29 (2005) 4–7.

[10] D. Hildebrandt, F. Gadelmeier, P. Grigull, K. McCormick, D. Naujoks, D. Sünder, Thermographic observation of the divertor target plates in the stellarators W7-AS and W7-X, J. Nucl. Mater. 313-316 (2003) 738–742.

[11] D. Hildebrandt, A. Dübner, H. Greuner, A. Wiltner, Thermal response to heat fluxes of the W7-AS divertor surface submitted to surface modification under high temperature treatment, J. Nucl. Mater. 390-391 (2009) 1118–1122.

[12] A. Rodatos, Algorithm development for safe operation of the Wendelstein 7-X divertor, Doctoral thesis, Technische Universität München, 2017. URL: http://nbn-resolving.de/urn/resolver.pl?urn:nbn:de:bvb:91-diss-20170331-1328685-0-8.

[13] D. Guilhem, J. Bondil, B. Bertrand, C. Desgranges, M. Lipa, P. Messina, M. Missirlian, C. Portafaix, R. Reichle, H. Roche, A. Saille, Tore-Supra infrared thermography system, a real steady-state diagnostic, Fusion Eng. Des. 74 (2005) 879–883.

[14] M. Mitteau, J. C. Vallet, R. Reichle, C. Brosset, P. Chappius, J. J. Cordier, E. Delchambre, F. Escourbiac, A. Grosman, D. Guilhem, M. Lipa, T. Loarer, J. Schlosser, E. Tsitrone, Evolution of carbon tiles during repetitive long pulse operation in Tore-Supra, Phys. Scr. T T111 (2004) 157–162.

[15] A. Herrmann, W. Junker, K. Günther, S. Bosch, M. Kaufmann, J. Neuhauser, G. Pautasso, T. Richter, R. Schneider, A. U. Team, Energy Flux to the ASDEX Upgrade Divertor Plates Determined by Thermography and Calorimetry, Plasma Phys. Control. Fusion 37 (1995) 17–29.

[16] A. Hermann, . ASDEX Upgrade Team, Limitations for divertor heat flux calculations of fast events in tokamaks, 28th EPS Conf. Control. Fusion Plasma Physics. Contrib. Pap. (2001) 2109–2112.

[17] B. Sieglin, M. Faitsch, A. Herrmann, B. Brucker, T. Eich, L. Kammerloher, S. Martinov, Real time capable infrared thermography for ASDEX Upgrade, Rev. Sci. Instrum. 86 (2015).

[18] P. Drewelow, Investigation of divertor heat flux pattern and their correlation to the edge magnetic field of the plasma confinement experiment LHD, Doctoral thesis, Technische Universität Berlin, Berlin, 2013. URL: https://depositonce.tu-berlin.de/handle/11303/4120. doi:http://dx.doi.org/10.14279/depositonce-3823.